

000 001 002 003 004 005 006 007 008 009 010 011 012 013 014 015 016 017 018 019 020 021 022 023 024 025 026 027 028 029 030 031 032 033 034 035 036 037 038 039 040 041 042 043 044 045 046 047 048 049 050 051 052 053 COMPREHEND AND TALK: TEXT TO SPEECH SYNTHESIS VIA DUAL LANGUAGE MODELING

005 **Anonymous authors**

006 Paper under double-blind review

ABSTRACT

011 Existing Large Language Model (LLM) based autoregressive (AR) text-to-speech
 012 (TTS) systems, while achieving state-of-the-art quality, still face critical chal-
 013 lenges. The foundation of this LLM-based paradigm is the discretization of the
 014 continuous speech waveform into a sequence of discrete tokens by neural audio
 015 codec. However, single codebook modeling is well suited to text LLMs, but suf-
 016 fers from significant information loss; hierarchical acoustic tokens, typically gen-
 017 erated via Residual Vector Quantization (RVQ), often lack explicit semantic struc-
 018 ture, placing a heavy learning burden on the model. Furthermore, the autoregres-
 019 sive process is inherently susceptible to error accumulation, which can degrade
 020 generation stability. To address these limitations, we propose CaT-TTS, a novel
 021 framework for robust and semantically-grounded zero-shot synthesis. First, we
 022 introduce S3Codec, a split RVQ codec that injects explicit linguistic features into
 023 its primary codebook via semantic distillation from a state-of-the-art ASR model,
 024 providing a structured representation that simplifies the learning task. Second, we
 025 propose an “Understand-then-Generate” dual-Transformer architecture that de-
 026 couples comprehension from rendering. An initial “Understanding” Transformer
 027 models the cross-modal relationship between text and the audio’s semantic tokens
 028 to form a high-level utterance plan. A subsequent “Generation” Transformer then
 029 executes this plan, autoregressively synthesizing hierarchical acoustic tokens. Fi-
 030 nally, to enhance generation stability, we introduce Masked Audio Parallel Infer-
 031 ence (MAPI), a nearly parameter-free inference strategy that dynamically guides
 032 the decoding process to mitigate local errors. Extensive experiments demonstrate
 033 that the synergy of our principled architecture and semantically-aware codec al-
 034 lows CaT-TTS to achieve new state-of-the-art performance in zero-shot voice
 035 cloning, with MAPI providing a measurable boost in generation robustness on
 036 benchmark datasets. Project page: <https://anonymous.4open.science/r/CaT-TTS-66A1>.

1 INTRODUCTION

037 Large Language Model (LLM) based autoregressive (AR) models have achieved state-of-the-art
 038 quality in zero-shot Text-to-Speech (TTS) with discrete audio representations (Wang et al., 2023; Du
 039 et al., 2024a;b; Anastassiou et al., 2024). With a few seconds of audio prompt, current TTS models
 040 are able to synthesize speech for any given text and mimic the speaker of the audio prompt. Contrary
 041 to NAR models (Chen et al., 2024b; Le et al., 2023), the sequential nature of AR models, where
 042 each acoustic token is conditioned on all its predecessors, naturally captures the long-range tempo-
 043 ral dependencies essential for rendering intricate intonation, rhythm, and emotional nuance. This
 044 sequential process synergizes perfectly with the in-context learning (ICL) capabilities of LLMs (Ye
 045 et al., 2025b; Wang et al., 2025b), providing a powerful mechanism for propagating the fine-grained
 046 acoustic characteristics of a voice prompt throughout a newly synthesized utterance.

047 Despite the remarkable progress in LLM-based zero-shot TTS, several fundamental challenges per-
 048 sist. The foundation of this LLM-based paradigm is the discretization of the continuous speech
 049 waveform into a sequence of discrete tokens, a task handled by a neural audio codec (Kreuk et al.,
 050 2022; Copet et al., 2023). Semantic tokens, typically derived from discretized self-supervised learn-
 051 ing (SSL) models, are considered to exhibit high alignment with text while leading to poor recon-
 052 struction (Du et al., 2024a; Ye et al., 2025a; Gong et al., 2025). In contrast, acoustic tokens often

054 derived from speech codecs trained through residual vector quantization GAN (RVQ-GAN), are
 055 recognized for capturing the details of the audio waveform, enabling high-quality synthesis, but
 056 lack explicit semantic grounding, forcing the LLM to learn the complex mapping from text to raw
 057 acoustic properties from scratch (Défossez et al., 2024; Kumar et al., 2023; Han et al., 2025). We
 058 assume that a better audio tokenizer should contain rich semantic information to facilitate an easy
 059 understanding of audio content, thus reducing the language model’s burden in interpreting tokens,
 060 and contains acoustic information for speech reconstruction. For better linguistic understanding and
 061 acoustic reconstruction, inspired by Mimi codec and SpeechTokenizer (Défossez et al., 2024; Zhang
 062 et al., 2023a), we propose S3Codec, a split residual vector quantization speech codec with semantic
 063 distillation. However, rather than using SSL models, we adopt a pretrained state-of-the-art ASR
 064 model for semantic distillation, which we assume brings more explicit linguistic features.

065 We argue that speech synthesis is fundamentally an information-increasing process, where a thor-
 066 ough understanding of the source conditions is a prerequisite for accurate and effective genera-
 067 tion (Chu et al., 2023; Xu et al., 2025; Xie & Wu, 2024). To embody this principle, we pro-
 068 pose CaT-TTS, a novel “Comprehend-and-Talk” text-to-speech framework, realized through a dual-
 069 transformer architecture that explicitly decouples contextual comprehension from acoustic ren-
 070 dering. Our first module, the Semantic Transformer, operates autoregressively on the semantic level.
 071 Its sole purpose is to model the rich interplay between the input text and the core semantic content
 072 of the voice prompt, building a holistic high-level representation, a latent “plan” for the entire ut-
 073 terance. Following this, our second module, the Acoustic Transformer, takes this contextual plan
 074 as its foundation and executes the synthesis. It generates the detailed acoustic tokens autoregres-
 075 sively. This design allows the model first to understand “what” and “how”, and then generates the
 076 “sound”, which dramatically reduces the modeling burden at each step, leading to more coherent
 077 and expressive output.

077 While our architectural design provides a more stable foundation, the challenge of long sequence
 078 lengths in speech remains (Zhang et al., 2023b; Le et al., 2023). Even with our proposed high
 079 compression ratio codec, which significantly shortens the acoustic token sequences, the risk of error
 080 accumulation persists in any AR system. To overcome this challenge, inspired by Classifier-Free
 081 Guidance (CFG) in diffusion models (Ho & Salimans, 2022) and Parallel Scaling Laws (Chen et al.,
 082 2025), we introduce Masked Audio Parallel Inference (MAPI). It constructs parallel computing
 083 streams with different masked audio tokens and aggregates these streams adaptively with learnable
 084 weights. This technique acts as a corrective mechanism, steering the model back on track when it
 085 begins to “hallucinate” and ensuring robust output.

086 In summary, we propose a novel zero-shot TTS system CaT-TTS powered by S3Codec. S3Codec
 087 encompasses acoustic and semantic information with low bit rates. Based on S3Codec, Cat-TTS
 088 embodies an understand and then generate rules via a dual language modeling strategy. To mitigate
 089 the error accumulation problem in audio language models, we introduce Masked Audio Parallel
 090 Inference strategy, which is beneficial for more robust token generation. Extensive experiments
 091 have shown that CaT-TTS has achieved a comparable or superior quality to existing models in terms
 092 of speech quality, similarity, and intelligibility.

093 2 RELATED WORK

094 **Speech Tokenization.** The success of autoregressive language models has spurred progress in
 095 speech LLMs, where speech tokenizers are essential for converting continuous signals into discrete
 096 tokens. Speech tokenizers are typically categorized as acoustic or semantic (Wang et al., 2025a;
 097 Yang et al., 2025). Acoustic tokens, optimized for signal reconstruction, capture detailed acoustic
 098 features beneficial for generation, but perform poorly on understanding tasks like ASR. Previous
 099 semantic tokenizers can be trained in two ways: (1) applying clustering or VQ to the representa-
 100 tions of self-supervised learning models (Zhang et al., 2023a; Défossez et al., 2024). (2) applying
 101 a VQ layer to the intermediate layer of ASR models (Du et al., 2024a;b). These semantic tokeniz-
 102 ers typically use a single codebook, have a simple architecture, are rich in linguistic information,
 103 and are well-suited for LLMs. However, finer-grained acoustic details such as pitch and prosody,
 104 are lost, resulting in poor performance on generation tasks (Łajszczak et al., 2024; Betker, 2023).
 105 An alternative for audio tokenization is to use multi-codebook residual vector quantization (RVQ).
 106 In RVQ, an audio frame is represented by a sum of vectors from several quantizers, allowing for

108 high-fidelity reconstruction over a range of bitrates by capturing details that single-codebook models
 109 often miss (Kumar et al., 2023; Défossez et al., 2022; Zeghidour et al., 2021). To align residual
 110 speech codec tokens with large text models, recent efforts have explored modeling both semantic
 111 and acoustic features simultaneously. SpeechTokenizer (Zhang et al., 2023a) enhances the RVQ-
 112 GAN paradigm with semantic distillation to guide the first layer of RVQ to align with a teacher SSL
 113 model. X-codec (Ye et al., 2025a) proposes an X-shaped structure where each layer of RVQ con-
 114 tains semantic and acoustic information. Mimi (Défossez et al., 2024) argues that distilling semantic
 115 information into the first level of a single RVQ will trade the audio quality restoration performance
 116 of the residual codebooks. Similar to Mimi, we propose S3Codec: a Split RVQ Speech Tokenizer
 117 with Semantic Distillation. Unlike Mimi, we adopt DAC architecture with pretrained Whisper for
 118 semantic distillation. This approach allows S3Codec to have good acoustic restoration ability and
 119 stronger linguistic information.

120 **LLM-based Zero-Shot TTS.** Inspired by the success of LLM, several recent works adopt language
 121 models to model text-to-speech (TTS) tasks (Chen et al., 2024a; Kharitonov et al., 2023; Meng
 122 et al., 2024). The LLM-based TTS systems are typically trained on tens of thousands of hours of
 123 speech data and have hundreds of millions of parameters, hence can leverage the emergent abil-
 124 ities of LLMs like in-context learning to enable zero-shot TTS. VALL-E pioneered treating TTS
 125 as a conditional language modeling problem by converting waveforms into neural codec tokens.
 126 Spear-TTS (Kharitonov et al., 2023) integrates multiple AR models to support multispeaker TTS
 127 with minimal supervision. Many systems use a single discrete codebook to quantize semantic fea-
 128 tures (Wang et al., 2025b; Ye et al., 2025b). Although simple, this bottleneck loses fine acoustic
 129 detail (Han et al., 2025). Recent TTS systems have often combined an AR language model with
 130 additional components (Du et al., 2024a), such as diffusion, to generate more natural, controllable
 131 speech when trained on large datasets. While these methods can produce high-quality results, most
 132 of them neglect the interactive understanding of speech and text modalities, instead requiring con-
 133 tinuous and fine-grained acoustic features for supplementation. Storing and processing such large-
 134 scale features is prohibitive, hindering training on hundreds of billions of tokens. In contrast, our
 135 approach utilizes a dual-autoregressive structure powered by a split RVQ discretization technique,
 136 with the first semantic transformer for modality understanding and the second acoustic transformer
 137 for acoustic information generation based on the context guide produced by the semantic trans-
 138 former. This understand-then-generate paradigm fits the natural flow of speech, takes advantage of
 139 the context learning of LLMs, and avoids the need for additional acoustic features for supplementary
 140 reconstruction.

141 3 METHOD

145 3.1 S3CODEC: SPLIT RVQ WITH SEMANTIC DISTILLATION FOR SPEECH TOKENIZER

147 To discretize waveforms into audio tokens, we introduce S3Codec, a neural audio codec that oper-
 148 ates as an autoencoder with a discrete bottleneck. Figure 2 shows the architecture. Based on the
 149 DAC architecture (Kumar et al., 2023), the encoder projects a single-channel waveform $\mathbf{x} \in \mathbb{R}^T$ to
 150 a latent representation $\mathbf{A} = \text{enc}(\mathbf{x}) \in \mathbb{R}^{L \times D}$ by cascading residual convolutional blocks that inter-
 151 leave dilated and strided convolutions along with Snake nonlinearities and weight normalizaton, and
 152 Quantizer quantize the latent representation to discrete representations $\mathbf{C} \in \mathbb{R}^{K \times L \times D}$ where L rep-
 153 resents the length of encoded tokens, K represents the number of codebooks and D represents the
 154 dimension of codebook. Similarly to SpeechTokenizer and Mimi, we distill semantic information
 155 into the first level of RVQ. However, instead of using SSL models like HuBERT (Hsu et al., 2021)
 156 as a semantic teacher, we adopt Whisper (Radford et al., 2023), a state-of-the-art model for auto-
 157 matic speech recognition and speech translation whose hidden representation contains rich explicit
 158 linguistic features. Mimi (Défossez et al., 2024) found that, while distillation significantly improves
 159 the phonetic discriminability of the first quantizer, it also negatively affects the audio quality. To
 160 address the issue, we split the RVQ layers in a way similar to Mimi. Rather than a single RVQ with
 161 K levels, we distill the semantic information into a plain VQ and apply an RVQ with $K - 1$ levels in
 162 parallel; thus the constraint of acoustic information being conserved in the residual of the semantic
 163 quantizer is removed.

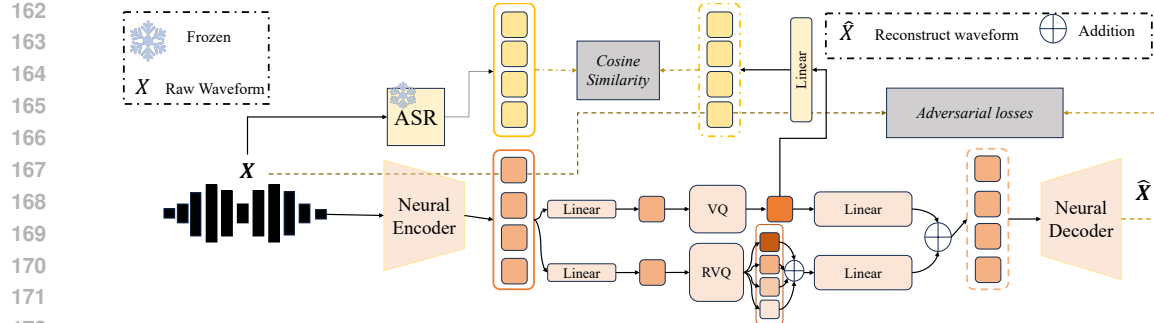


Figure 1: S3Codec architecture overview.

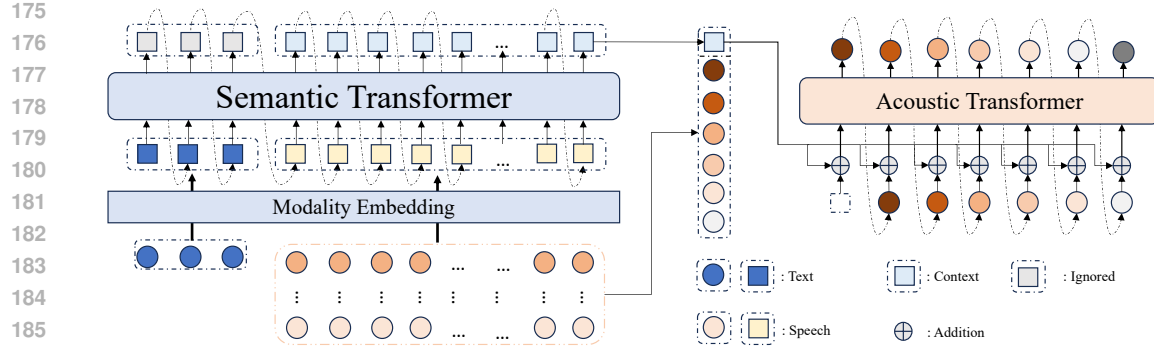


Figure 2: An overview of CaT-TTS architecture. Semantic Transformer models the temporal context information, while Acoustic Transformer models the acoustic information from coarse to fine.

3.1.1 TRAINING OBJECTIVE

S3Codec is trained with the combination of reconstruction, semantic distillation and adversarial losses. Reconstruction and adversarial losses can be found in Appendix E. For semantic distillation task, we calculated the cosine distance between the output of the first quantizer and the transformed Whisper embeddings, which is denoted as $\cos(\cdot)$, to perform distillation. Formally, the distillation loss is defined as follows:

$$\mathcal{L}_{distill} = 1 - \frac{1}{L} \sum_{t=1}^L \cos(\mathbf{C}_t^0, \text{Proj}(\mathbf{E}^S)_t), \quad (1)$$

where $\mathbf{C}_t^0 \in \mathbb{R}^D$ represents the first encoded embeddings for the frame t , $\mathbf{E}^S \in \mathbb{R}^{L_S \times D_S}$ represents the semantic embeddings obtained from the Whisper Encoder, $\text{Proj}(\cdot) : \mathbb{R}^{L_S \times D_S} \rightarrow \mathbb{R}^{L \times D}$ represents the projection operation that maps whisper latent embedding to the space of audio embedding, L_S represents the length of semantic frames, and $\text{Proj}(\mathbf{E}^S)_t$ represents the projected whisper embedding for frame t . The details of the overall training objective are listed in the Appendix C.

3.2 DUAL LANGUAGE MODELING OF AUDIO TOKENS

3.2.1 PROBLEM FORMULATION

Given a dataset $\mathcal{D} = \{\mathbf{x}, \mathbf{y}\}$, where \mathbf{y} is an audio sample and \mathbf{x} is the corresponding text transcription. We use a pre-trained neural codec model to encode each audio sample into discrete codes, denoted as $\text{S3Codec}(\mathbf{y}) = \mathbf{A} \in \mathbb{R}^{K \times L}$, where K represents the number of codebooks, and L is the downsampled utterance length. $\mathbf{A}_t \in \mathbb{R}^K$ represents the K codes for frame t and \mathcal{A}_t^k represents the code for the k -th codebook of frame t . Mathematically, given the text prompt \mathcal{T} and the speech prompt $\tilde{\mathbf{A}}$, our target is to train a neural language model to generate the discrete code matrix \mathbf{A} with the optimization objective of maximizing the distribution:

$$\mathbb{P}(\mathbf{A}|\mathcal{T}, \tilde{\mathbf{A}}). \quad (2)$$

To build such a model, we propose a dual auto-regressive Transformer modeling framework. The dual auto-regressive (AR) Transformer models the residual vector quantization (RVQ) output as a two-level autoregressive process, operating first along the temporal axis and subsequently across codebooks. The core intuition behind this design is to preserve both the causal nature of speech generation and the hierarchical refinement characteristic of RVQ. We denote the first transformer as the semantic transformer, following the causal nature of speech generation and context learning, while the second transformer is the acoustic transformer, modeling the acoustic feature in a coarse-to-fine manner.

3.2.2 SEMANTIC TRANSFORMER

The semantic transformer functions as a thinker responsible for processing and understanding the text and the audio modality, and generating high-level representations. Mathematically, let $\mathcal{T} \in \mathbb{R}^M$ represent the tokenized textual prompt, $\mathbf{A} \in \mathbb{R}^{K \times L}$ represent the corresponding speech, and $\mathbf{A}^i \in \mathbb{R}^L, i = \{0, \dots, K-1\}$ represent the speech codes in the i -th codebook, where M represents the length of the encoded text token and L represents the length of the encoded speech token. Given tokenized text prompt and encoded prompt audio codes, the semantic transformer learns the linguistic features of the text \mathcal{T} and the discrete acoustic representation of the prompt audio $\tilde{\mathbf{A}}$ and outputs a latent feature \mathbf{H}^{ctx} as a guide for the generation of subsequent speech tokens. The optimization objective of the semantic transformer is maximizing the distribution:

$$\mathbb{P}(\mathbf{H}^{ctx} | \mathcal{T}, \tilde{\mathbf{A}}; \theta_S) = \prod_{t=1}^L \mathbb{P}(\mathbf{H}_t^{ctx} | \mathcal{T}, \mathbf{H}_{<t}^{ctx}, \tilde{\mathbf{A}}; \theta_S). \quad (3)$$

Speech Token Sequence Modeling. To be able to inject discrete speech representations into LLM, some research proposes to use a single codebook codec to make the speech modality well adapted in the way of text tokens. CaT-TTS fits the RVQ paradigm and, specifically, the multiple codebook information at each time step will be aggregated as the speech representation of the current time step. Thus, at each time step t , the audio representation can be formulated as $\mathbf{S}_t = \sum_{i=0}^{K-1} \mathcal{A}_t^i$, where \mathcal{A}_t^i represents the i -th encoded representation for frame t .

Next Token Embedding Prediction. In order to inject RVQ speech representation into LLM, we sum the codebook dimensions of the multi-codebook parallel sequence. Aggregation brings rich linguistic and acoustic content to the semantic transformer; however, the speech representation of each time step is no longer a quantitative representation. To solve this problem, we propose direct embedding prediction. Instead of predicting discrete token IDs and computing cross-entropy loss, we directly predict the next embedding vector in the continuous semantic space and optimize using Mean Squared Error Loss between predicted and target embeddings. Specifically, our model learns to predict the next semantic embedding as $\mathbf{H}_{t+1}^{ctx} = \theta_S(\mathbf{H}_1^{ctx}, \mathbf{H}_2^{ctx}, \dots, \mathbf{H}_t^{ctx})$, where \mathbf{H}_t^{ctx} represents the continuous semantic embedding at position t . To be more task-specific, we denote $\mathbf{H}^{ctx} \doteq (\mathbf{T} \oplus \mathbf{S})$, where \mathbf{T} represents the text modality, \mathbf{S} represents the audio modality, and \oplus represents the concatenate operation. We split the high-level representation and focus on speech modality; thus the optimization objective can be formulated as follows:

$$\mathbb{P}(\mathbf{H}^{ctx} | \mathcal{T}, \tilde{\mathbf{A}}; \theta_S) = \mathbb{P}(\mathbf{S} | \mathcal{T}, \tilde{\mathbf{A}}; \theta_S) = \prod_{t=1}^{L_{|S|}} \mathbb{P}(\mathbf{S}_t | \mathcal{T}, \mathbf{S}_{<t}, \tilde{\mathbf{A}}; \theta_S), \quad (4)$$

where $L_{|S|}$ represents the length of speech frames, as the text tokens are ignored. To achieve this, we replace the standard cross-entropy loss with MSE loss to handle continuous targets:

$$\mathcal{L}_{ctx} = - \sum_{t=1}^{L_{|S|}} \log \mathbb{P}(\mathbf{S}_t | \mathcal{T}, \mathbf{S}_{<t}, \tilde{\mathbf{A}}; \theta_S) \rightarrow \mathcal{L}_{ctx} = \sum_{t=1}^{L_{|S|}} \|\mathbf{S}_t - \theta_S(\mathbf{S}_{<t}, \mathcal{T}, \tilde{\mathbf{A}})\|_2. \quad (5)$$

3.2.3 ACOUSTIC TRANSFORMER

The purpose of the acoustic transformer is to reconstruct discrete speech representations from coarse-grained to fine-grained based on the learned preceding text and speech modal information. The optimization objective of the acoustic transformer is maximizing the following distribution:

$$\mathbb{P}(\mathbf{A}_t | \mathbf{S}_t; \theta_A) = \prod_{k=0}^{K-1} \mathbb{P}(\mathcal{A}_t^k | \mathcal{A}_t^{<k}, \mathbf{S}_t; \theta_A). \quad (6)$$

270
 271 Table 1: Objective Evaluation Metrics for Comparison with Baseline Codecs. S-T represents
 272 SpeechTokenizer for simplicity.

273	Tokenizer	CB	Nq	FR	BR (bps)	PESQ \uparrow	STOI \uparrow	STFT \downarrow	Mel \downarrow	SIM \uparrow
274	Encodec	1024	8	75Hz	6k	2.76	0.94	0.11	2.13	0.89
275	DAC-8	1024	8	75Hz	6k	3.46	0.95	0.06	2.02	0.96
276	S-T	1024	8	50Hz	4k	2.66	0.92	0.59	7.07	0.84
277	Encodec-2	1024	2	75Hz	1.5k	1.56	0.94	0.23	4.45	0.90
278	DAC-2	1024	2	75Hz	1.5k	1.51	0.83	0.12	3.36	0.49
279	BigCodec	8192	1	80Hz	1.04k	2.68	0.93	-	-	0.84
280	Xcodec	1024	2	50Hz	1k	2.33	0.87	-	-	0.72
281	S-T	1024	2	50Hz	1k	1.25	0.77	0.68	8.02	0.36
282	Mimi	2048	8	12.5Hz	1.1k	2.24	0.90	-	-	0.73
283	MBCodec	2048	8	25Hz	2.2k	2.98	0.94	0.17	3.62	0.87
284	S3Codec	4096	8	12.5Hz	1.2k	2.85	0.94	0.12	4.01	0.89

285
 286 The combination of the semantic transformer and the acoustic transformer can guide the generation
 287 of target audio through the understanding of text and speech modalities, which conforms to the
 288 objective laws of human speech production. Finally, the overall optimization objective Eq.2 can be
 289 detailed as:

$$290 \quad \mathbb{P}(\mathbf{A}|\mathcal{T}, \tilde{\mathbf{A}}) = \prod_{t=1}^{L_{|\mathcal{S}|}} \left[\mathbb{P}(\mathbf{S}_t|\mathbf{S}_{<t}, \mathcal{T}, \tilde{\mathbf{A}}; \theta_{\mathcal{S}}) \cdot \prod_{k=0}^{K-1} \mathbb{P}(\mathcal{A}_t^k|\mathcal{A}_t^{<k}, \mathbf{S}_t; \theta_{\mathcal{A}}) \right]. \quad (7)$$

293 Consequently, the overall goal of training optimization objective is fourmulated as follows:

$$295 \quad \mathcal{L}_{total} = \sum_{t=1}^{L_{|\mathcal{S}|}} \left[\|\mathbf{S}_t - \theta_{\mathcal{S}}(\mathbf{S}_{<t}, \mathcal{T}, \tilde{\mathbf{A}})\|_2 - \sum_{k=0}^{K-1} \log \mathbb{P}(\mathcal{A}_t^k|\mathcal{A}_t^{<k}, \mathbf{S}_t; \theta_{\mathcal{A}}) \right]. \quad (8)$$

298 The mathematical derivation can be found in the Appendix D.

300 3.3 MASKED AUDIO PARALLEL INFERENCE

302 Due to the uncertainty of each token prediction, especially in speech generation, errors accumulate,
 303 which reduces the expressiveness of the generated speech. To address this challenge, inspired
 304 by (Chen et al., 2025), we introduce Masked Audio Parallel Scaling in the semantic generation
 305 module. Specifically, for each prompt token sequence, we duplicate it P times and apply a masking
 306 strategy to speech tokens separately with a certain probability, resulting in a total of P token
 307 sequences. The model then produces P output sequences, and these P candidates are weighted
 308 and summed with a learnable weight to produce the final output sequence. Formally, in our speech
 309 generation task, the discrete text token embeddings and audio embeddings will be concatenated,
 310 resulting in the input embeddings, denoted as $\mathbf{x} \in \mathbb{R}^{L_{in} \times D}$. Specifically, we denote our trained
 311 semantic transformer $\theta_{\mathcal{S}} : \mathbb{R}^{L_{in} \times D} \rightarrow \mathbb{R}^{L_{in} \times D}$, where θ is the parameter, L_{in} is the length of
 312 input text and audio embeddings and D is the model dimension, the final output is formulated in the
 313 following form:

$$314 \quad \theta_{\mathcal{S}}^*(\mathbf{x}) = w_1 \theta_{\mathcal{S}}(\mathbf{z}_1) + w_2 \theta_{\mathcal{S}}(\mathbf{z}_2) + \cdots + w_P \theta_{\mathcal{S}}(\mathbf{z}_P), \quad (9)$$

315 where P denotes the number of parallel streams, $\mathbf{z}_1, \dots, \mathbf{z}_P$ are P distinct mask transformations
 316 of \mathbf{x} , and w_1, \dots, w_P are adaptive-trained aggregation weights. More details can be found in the
 317 Appendix B.

319 4 EXPERIMENTS

321 4.1 AUDIO QUANTIZATION AND RECONSTRUCTION ANALYSIS

323 S3Codec is trained on the subset of our amassed speech data. Implementation details are listed in
 Appendix E.

324

325

Table 2: Objective evaluation in the SeedTTS test datasets.

326

327

Model	test-zh		test-en		test-hard	
	WER(%) ↓	SIM ↑	WER(%) ↓	SIM ↑	WER(%) ↓	SIM ↑
NAR-involved Models						
MaskGCT	2.27	0.774	2.62	0.714	10.27	0.748
E2 TTS (32 NFE)	1.97	0.730	2.19	0.710	-	-
F5-TTS (32 NFE)	1.56	0.741	1.83	0.647	8.67	0.713
Seed-TTS	1.12	0.796	2.25	0.762	7.59	0.776
FireRedTTS	1.51	0.635	3.82	0.460	17.45	0.621
CosyVoice	3.63	0.723	4.29	0.609	11.75	0.709
CosyVoice 2	1.45	0.748	2.57	0.652	6.83	0.724
CosyVoice 3-0.5B	1.16	0.780	2.02	0.718	6.08	0.758
Pure AR based Models						
QTTS	1.66	0.648	3.17	0.652	14.45	0.641
Spark-TTS	1.20	0.672	1.98	0.584	-	-
Llasa-1B-250k	1.89	0.668	3.22	0.572	12.13	0.638
Llasa-3B-250k	1.60	0.675	3.14	0.579	13.37	0.652
Llasa-8B-250k	1.59	0.684	2.97	0.574	11.09	0.660
CaT-TTS	1.56	0.678	2.35	0.668	9.75	0.674

336

337

Baselines. To assess the reconstruction performance of S3Codec, we employ several state-of-the-art neural codecs as baselines, including Encodec (Défossez et al., 2022), DAC (Kumar et al., 2023), QDAC (Han et al., 2025), SpeechTokenizer (Zhang et al., 2023a), BigCodec (Xin et al., 2024), Xcodec (Ye et al., 2025a) and MBCodec (Zhang et al., 2025).

344

Evaluation Metrics. To evaluate the performance of S3Codec, we employ several metrics, including SIM, STFT Distance, Mel Distance, short-time objective intelligibility (STOI) (Taal et al., 2010) and perceptual evaluation of speech quality (PESQ) (Rix et al., 2001). All evaluations were conducted on the LibriSpeech (Panayotov et al., 2015) test-clean subset. More detailed evaluation set up is listed in Appendix E.2.

354

Evaluation Results. As shown in Table 4, S3Codec achieves SOTA-comparable performance with a very low frame rate in most evaluation dimensions. S3codec achieves higher SIM scores than MBcodec, Mimi, and SpeechTokenizer with the same codebooks. In terms of the restoration and perception indicators PESQ and STOI, S3codec is comparable to the high bitrates Encodec and DAC-8. At the evaluation dimension of STFT and Mel indicators, S3Codec also performs well among low-bitrate codecs. These results provide preliminary evidence of the model’s effectiveness in reconstructing speech. As for the semantic evaluation, results in the Appendix E.2 demonstrate the superiority of S3Codec.

362

363

4.2 ZERO-SHOT TTS PERFORMANCE

364

365

Datasets. To train the CaT-TTS models, we have amassed a considerable dataset comprising multiple languages. The dataset contains about 200k hours labeled speech, with about 85% Chinese data and 15% English data. We evaluate our zero-shot TTS models with five benchmarks: (1) Seed-TTS test-en, a test set introduced in Seed-TTS of sample extracted from English public corpora, includes 1,000 samples from the Common Voice dataset. (2) SeedTTS test-zh, a test set introduced in Seed-TTS of samples extracted from Chinese public corpora, includes 2,020 samples from the DiDiSpeech (Guo et al., 2021) dataset. (3) Seed-TTS test-hard, includes 400 samples that consist of complex Chinese sentences. (4) PGC-Hard, includes 1500 Chinese samples, containing Professionally-Generated Content. (5) PGC-Poly, includes 1500 Chinese samples, containing polyphonic characters. The PGC testset is specially designed to test model generalization on difficult, out-of-domain voices.

374

375

376

377

Evaluation Metrics. We adopt the word error rate (WER) and speaker similarity (SIM) metrics for objective evaluation. For WER, we employ Whisper-large-v3 (Radford et al., 2023) and Paraformer-zh (Gao et al., 2023) as the automatic speech recognition engines for English and Mandarin, respectively. For SIM, we use WavLM-large fine-tuned on the speaker verification task to obtain

Table 3: Objective evaluation on hard mandarin test. \dagger represents the self-implemented model. — means the average evaluation results across three sets.

Model	Model Size	WER(%) ↓		PGC-Poly	SIM↑	UTMOS↑
		Seed-Hard	PGC-Hard		-	-
CosyVoice	0.3B	11.75	7.86	16.22	0.709	3.01
CosyVoice 2	0.5B	6.83	6.11	14.25	0.713	3.02
L-CosyVoice50 [†]	0.2B	9.52	8.15	18.71	0.691	2.92
L-CosyVoice25 [†]	0.5B	7.46	6.83	13.84	0.706	2.99
Q-TTS	0.2B	14.45	7.89	14.37	0.654	3.03
VALL-E [†]	0.2B	13.12	9.68	15.71	0.631	3.05
CaT-TTS	0.4B	9.75	7.03	13.97	0.672	3.13

speaker embeddings used to calculate the cosine similarity of speech samples of each test utterance against reference clips. For naturalness, we use SpeechMOS MOS prediction model to calculate UTMOS (Saeki et al., 2022) scores for evaluation.

Baselines. We compare our models with state-of-the-art zero-shot TTS systems, including Seed-TTS (Anastassiou et al., 2024), FireRedTTS (Guo et al., 2024), MaskGCT (Wang et al., 2024), E2 TTS (Eskimez et al., 2024), F5-TTS (Chen et al., 2024b), CosyVoice (Du et al., 2024a), CosyVoice2 (Du et al., 2024b), VALL-E (Wang et al., 2023) and QTTS (Han et al., 2025). Details of each model can be found in the Appendix F.2. In particular, we also compare the performance of SOTA two-stage models, including VALL-E, CosyVoice, CosyVoice 2, QTTS and self-implement AR (Llama) (Dubey et al., 2024) + flow-matching models (Lipman et al., 2022), where L-CosyVoice50 means Llama backbone with 50 Hz semantic codec (Hsu et al., 2021) and L-CosyVoice25 means with 25 Hz.

Training. We train CaT-TTS on 8 NVIDIA H20 96GB GPUs. The parallel stream is set to 4. For more details about the model architecture, please refer to Appendix F.1. We optimize the model with the AdamW optimizer with a learning rate of 1e-5 and 20K warm-up steps.

Evaluation Results. To evaluate CaT-TTS’s zero-shot TTS capability, we assess its performance on Seed-TTS-eval and compare it with existing zero-shot TTS models. These experiments focus on cross-sentence speaker similarity and the generation of intelligible speech. The results are presented in Table 4.1. As can be seen, CaT-TTS demonstrates a significant superiority in intelligibility for zero-shot TTS scenarios. With WER 1.56%, 2.35% and 9.75% in test-zh, test-en and test-hard, respectively, CaT-TTS achieves best or best comparable performance among these baselines, especially in pure AR based models. In terms of speaking similarity, like the other Pure AR based models, Cat-TTS’s performance is inferior to NAR-involved models, especially pure NAR models. The reason is that NAR models like F5-TTS generate based on more explicit acoustic features like Mel-Spectrogram, and AR+NAR models typically construct acoustic information with acoustic guidance like speaker similarity vector in the NAR stage. Although with higher indicator performance, we think it may degrade diversity and cause more storage and processing cost during training. To do a further comprehensive comparison on zero-shot TTS performance, we compared recent prominent AR-based two-stage TTS models including VALL-E, CosyVoice, QTTS and reproduced Llama-CosyVoice as baseline models, and testify the synthesis capability in a more real scenarios. The evaluation datasets including PGC-Hard and PGC-Poly, which contain more complex real-life sentences and polyphonetic characters, respectively. The results in Table 4.2 demonstrate that CaT-TTS has SOTA comparable in-context learning ability. With WER 9.75%, 7.03% and 13.97% in Seed-TTS test-zh-hard, PGC-Hard and PGC-Poly, respectively. Q-TTS and VALL-E are Transformer-based TTS systems powered by codec, which is similar to CaT-TTS. As can be seen, CaT-TTS achieves better performance. Although without additional acoustic information supplement through flow-matching, CaT-TTS has comparable or superior performance in terms of UTMOS and WER, demonstrating the context-learning ability of our system.

4.3 ABLATION STUDY

Modality UnderStanding. To demonstrate the effectiveness and superiority of the modality understanding loss. We trained two models in sub-dataset with the same architecture but with small model

432
433
434

Table 4: Objective Evaluation. Comparison between models trained with and without semantic guidance.

435
436
437
438
439

Model	WER(%) ↓			SIM↑	UTMOS ↑
	SeedTTS-test	PGC-Hard	PGC-Poly	-	-
CaT-TTS w/o	3.97	11.83	18.34	0.649	2.64
CaT-TTS	3.31	9.74	16.57	0.658	2.78

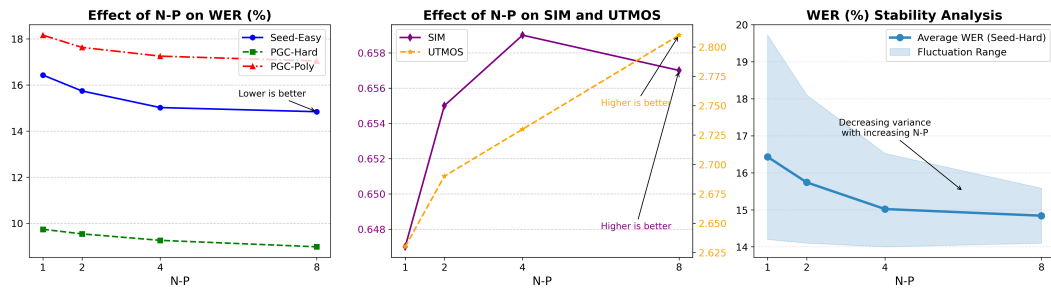
440
441
442
443
444
445
446
447
448
449450
451
452
453

Figure 3: The result analysis of number of parallel streams.

454
455
456
457
458
459
460
461

size, and one of them is trained without semantic guidance. Table 4.2 shows the comparison results. With the loss of semantic guidance removed, this leads to performance decreases, especially with the WER increasing from 3.31% to 3.97% in SeedTTS-test, 9.74% to 11.83% in PGC-Hard and 16.57% to 18.34% in PGC-Poly, and the speech quality indicators SIM and UTMOS have also been reduced. During model training, semantic loss forces the semantic transformer to enhance its understanding of text and semantic modalities, thus improving the linguistic understanding ability of CaT-TTS. These results underscore the pivotal role of semantic loss in ensuring accurate semantic information learning, which is essential for maintaining high-fidelity generation of acoustic transformer.

462
463
464
465
466
467
468
469
470
471
472
473

Masked Audio Parallel Inference. To evaluate the effectiveness of masked parallel inference, we trained CaT-TTS-small in the subset of the collected dataset. We set different parallel streams and evaluated the performance in the PGC-Hard, PGC-Poly, and SeedTTS test-zh-easy dataset. Results in Figure 4 show the average performance analysis of MAPI parallel streams. The left subfigure shows the speech intelligibility improvement that MAPI brings. The middle subfigure shows that as the number of parallel streams increases, the acoustic performance SIM score and the UTMOS score show an upward trend. To demonstrate the robustness of MAPI, each sample in these datasets will be evaluated 10 times. As can be seen in the right subfigure in Figure 4, the performance of each inference is more stable in terms of the WER indicator. Due to the parallel computing capability of GPU, MAPI almost does not bring additional time consumption, but as the number of parallel streams increases, the utilization of GPU resources also increases. It is necessary to select the most appropriate number of parallel streams according to the requirements of the actual scenario.

474
475

5 CONCLUSION

476
477
478
479
480
481
482
483
484
485

In this work, we introduced CaT-TTS, a novel Text-to-Speech system designed to address key challenges in representation and generation. At its core is S3Codec, a split RVQ codec that resolves the trade-off between reconstruction fidelity and semantic interpretability by injecting linguistic features via ASR-based distillation. Building on this semantically aware representation, we proposed a principled “Understand-then-Generate” paradigm, realized through a dual-Transformer architecture that decouples contextual comprehension from acoustic rendering. To complement this, we developed Masked Audio Parallel Inference (MAPI), a nearly parameter-free inference strategy that enhances generation stability by dynamically mitigating local decoding errors. Extensive experiments demonstrate that the synergy between our architecture and codec allows CaT-TTS to achieve state-of-the-art performance in zero-shot voice cloning, with MAPI providing a measurable boost in robustness on benchmark datasets.

486 REFERENCES
487

488 Philip Anastassiou, Jiawei Chen, Jitong Chen, Yuanzhe Chen, Zhuo Chen, Ziyi Chen, Jian Cong,
489 Lelai Deng, Chuang Ding, Lu Gao, et al. Seed-tts: A family of high-quality versatile speech
490 generation models. *arXiv preprint arXiv:2406.02430*, 2024.

491 James Betker. Better speech synthesis through scaling. *arXiv preprint arXiv:2305.07243*, 2023.
492

493 Mouxiang Chen, Binyuan Hui, Zeyu Cui, Jiaxi Yang, Dayiheng Liu, Jianling Sun, Junyang Lin, and
494 Zhongxin Liu. Parallel scaling law for language models. *arXiv preprint arXiv:2505.10475*, 2025.

495 Sanyuan Chen, Shujie Liu, Long Zhou, Yanqing Liu, Xu Tan, Jinyu Li, Sheng Zhao, Yao Qian, and
496 Furu Wei. Vall-e 2: Neural codec language models are human parity zero-shot text to speech
497 synthesizers. *arXiv preprint arXiv:2406.05370*, 2024a.

498 Yushen Chen, Zhikang Niu, Ziyang Ma, Keqi Deng, Chunhui Wang, Jian Zhao, Kai Yu, and Xie
499 Chen. F5-tts: A fairytaler that fakes fluent and faithful speech with flow matching. *arXiv preprint
500 arXiv:2410.06885*, 2024b.

501 Yunfei Chu, Jin Xu, Xiaohuan Zhou, Qian Yang, Shiliang Zhang, Zhijie Yan, Chang Zhou, and
502 Jingren Zhou. Qwen-audio: Advancing universal audio understanding via unified large-scale
503 audio-language models. *arXiv preprint arXiv:2311.07919*, 2023.

504 Jade Copet, Felix Kreuk, Itai Gat, Tal Remez, David Kant, Gabriel Synnaeve, Yossi Adi, and Alexandre Défossez.
505 Simple and controllable music generation. *Advances in Neural Information Processing Systems*, 36:47704–47720, 2023.

506 Alexandre Défossez, Jade Copet, Gabriel Synnaeve, and Yossi Adi. High fidelity neural audio
507 compression. *arXiv preprint arXiv:2210.13438*, 2022.

508 Alexandre Défossez, Laurent Mazaré, Manu Orsini, Amélie Royer, Patrick Pérez, Hervé Jégou,
509 Edouard Grave, and Neil Zeghidour. Moshi: a speech-text foundation model for real-time dia-
logue. *arXiv preprint arXiv:2410.00037*, 2024.

510 Zhihao Du, Qian Chen, Shiliang Zhang, Kai Hu, Heng Lu, Yexin Yang, Hangrui Hu, Siqi Zheng, Yue
511 Gu, Ziyang Ma, et al. Cosyvoice: A scalable multilingual zero-shot text-to-speech synthesizer
512 based on supervised semantic tokens. *arXiv preprint arXiv:2407.05407*, 2024a.

513 Zhihao Du, Yuxuan Wang, Qian Chen, Xian Shi, Xiang Lv, Tianyu Zhao, Zhifu Gao, Yexin Yang,
514 Changfeng Gao, Hui Wang, et al. Cosyvoice 2: Scalable streaming speech synthesis with large
515 language models. *arXiv preprint arXiv:2412.10117*, 2024b.

516 Zhihao Du, Changfeng Gao, Yuxuan Wang, Fan Yu, Tianyu Zhao, Hao Wang, Xiang Lv, Hui Wang,
517 Chongjia Ni, Xian Shi, et al. Cosyvoice 3: Towards in-the-wild speech generation via scaling-up
518 and post-training. *arXiv preprint arXiv:2505.17589*, 2025.

519 Abhimanyu Dubey, Abhinav Jauhri, Abhinav Pandey, Abhishek Kadian, Ahmad Al-Dahle, Aiesha
520 Letman, Akhil Mathur, Alan Schelten, Amy Yang, Angela Fan, et al. The llama 3 herd of models.
521 *arXiv e-prints*, pp. arXiv–2407, 2024.

522 Sefik Emre Eskimez, Xiaofei Wang, Manthan Thakker, Canrun Li, Chung-Hsien Tsai, Zhen Xiao,
523 Hemin Yang, Zirun Zhu, Min Tang, Xu Tan, et al. E2 tts: Embarrassingly easy fully non-
524 autoregressive zero-shot tts. In *2024 IEEE Spoken Language Technology Workshop (SLT)*, pp.
525 682–689. IEEE, 2024.

526 Zhifu Gao, Zerui Li, Jiaming Wang, Haoneng Luo, Xian Shi, Mengzhe Chen, Yabin Li, Lingyun
527 Zuo, Zhihao Du, Zhangyu Xiao, et al. Funasr: A fundamental end-to-end speech recognition
528 toolkit. *arXiv preprint arXiv:2305.11013*, 2023.

529 Yitian Gong, Luozhijie Jin, Ruifan Deng, Dong Zhang, Xin Zhang, Qinyuan Cheng, Zhaoye Fei,
530 Shimin Li, and Xipeng Qiu. Xy-tokenizer: Mitigating the semantic-acoustic conflict in low-bitrate
531 speech codecs. *arXiv preprint arXiv:2506.23325*, 2025.

540 Hao-Han Guo, Yao Hu, Kun Liu, Fei-Yu Shen, Xu Tang, Yi-Chen Wu, Feng-Long Xie, Kun Xie,
 541 and Kai-Tuo Xu. Fireredtts: A foundation text-to-speech framework for industry-level generative
 542 speech applications. *arXiv preprint arXiv:2409.03283*, 2024.

543

544 Tingwei Guo, Cheng Wen, Dongwei Jiang, Ne Luo, Ruixiong Zhang, Shuaijiang Zhao, Wubo Li,
 545 Cheng Gong, Wei Zou, Kun Han, et al. Didispeech: A large scale mandarin speech corpus. In
 546 *ICASSP 2021-2021 IEEE International Conference on Acoustics, Speech and Signal Processing*
 547 (*ICASSP*), pp. 6968–6972. IEEE, 2021.

548

549 Yichen Han, Xiaoyang Hao, Keming Chen, Weibo Xiong, Jun He, Ruonan Zhang, Junjie Cao, Yue
 550 Liu, Bowen Li, Dongrui Zhang, et al. Quantize more, lose less: Autoregressive generation from
 551 residually quantized speech representations. *arXiv preprint arXiv:2507.12197*, 2025.

552

553 Jonathan Ho and Tim Salimans. Classifier-free diffusion guidance. *arXiv preprint*
 554 *arXiv:2207.12598*, 2022.

555

556 Wei-Ning Hsu, Benjamin Bolte, Yao-Hung Hubert Tsai, Kushal Lakhotia, Ruslan Salakhutdinov,
 557 and Abdelrahman Mohamed. Hubert: Self-supervised speech representation learning by masked
 558 prediction of hidden units. *IEEE/ACM transactions on audio, speech, and language processing*,
 29:3451–3460, 2021.

559

560 Eugene Kharitonov, Damien Vincent, Zalán Borsos, Raphaël Marinier, Sertan Girgin, Olivier
 561 Pietquin, Matt Sharifi, Marco Tagliasacchi, and Neil Zeghidour. Speak, read and prompt: High-
 562 fidelity text-to-speech with minimal supervision. *Transactions of the Association for Computa-*

563

564 *tional Linguistics*, 11:1703–1718, 2023.

565

566 Felix Kreuk, Gabriel Synnaeve, Adam Polyak, Uriel Singer, Alexandre Défossez, Jade Copet, Devi
 567 Parikh, Yaniv Taigman, and Yossi Adi. Audiogen: Textually guided audio generation. *arXiv*
 568 *preprint arXiv:2209.15352*, 2022.

569

570 Rithesh Kumar, Prem Seetharaman, Alejandro Luebs, Ishaan Kumar, and Kundan Kumar. High-
 571 fidelity audio compression with improved rvqgan. *Advances in Neural Information Processing*
 572 *Systems*, 36:27980–27993, 2023.

573

574 Mateusz Łajszczak, Guillermo Cámbara, Yang Li, Fatih Beyhan, Arent Van Korlaar, Fan Yang,
 575 Arnaud Joly, Álvaro Martín-Cortinas, Ammar Abbas, Adam Michalski, et al. Base tts: Lessons
 576 from building a billion-parameter text-to-speech model on 100k hours of data. *arXiv preprint*
 577 *arXiv:2402.08093*, 2024.

578

579 Matthew Le, Apoorv Vyas, Bowen Shi, Brian Karrer, Leda Sari, Rashel Moritz, Mary Williamson,
 580 Vimal Manohar, Yossi Adi, Jay Mahadeokar, et al. Voicebox: Text-guided multilingual universal
 581 speech generation at scale. *Advances in neural information processing systems*, 36:14005–14034,
 2023.

582

583 Jae Hyun Lim and Jong Chul Ye. Geometric gan. *arXiv preprint arXiv:1705.02894*, 2017.

584

585 Yaron Lipman, Ricky TQ Chen, Heli Ben-Hamu, Maximilian Nickel, and Matt Le. Flow matching
 586 for generative modeling. *arXiv preprint arXiv:2210.02747*, 2022.

587

588 Lingwei Meng, Long Zhou, Shujie Liu, Sanyuan Chen, Bing Han, Shujie Hu, Yanqing Liu, Jinyu
 589 Li, Sheng Zhao, Xixin Wu, et al. Autoregressive speech synthesis without vector quantization.
 590 *arXiv preprint arXiv:2407.08551*, 2024.

591

592 Vassil Panayotov, Guoguo Chen, Daniel Povey, and Sanjeev Khudanpur. Librispeech: an asr corpus
 593 based on public domain audio books. In *2015 IEEE international conference on acoustics, speech*
 and signal processing (ICASSP), pp. 5206–5210. IEEE, 2015.

594

595 Alec Radford, Jong Wook Kim, Tao Xu, Greg Brockman, Christine McLeavey, and Ilya Sutskever.
 596 Robust speech recognition via large-scale weak supervision. In *International conference on ma-*
 597 *chine learning*, pp. 28492–28518. PMLR, 2023.

594 Antony W Rix, John G Beerends, Michael P Hollier, and Andries P Hekstra. Perceptual evaluation
 595 of speech quality (pesq)-a new method for speech quality assessment of telephone networks and
 596 codecs. In *2001 IEEE international conference on acoustics, speech, and signal processing. Proceedings (Cat. No. 01CH37221)*, volume 2, pp. 749–752. IEEE, 2001.

598 Takaaki Saeki, Detai Xin, Wataru Nakata, Tomoki Koriyama, Shinnosuke Takamichi, and Hi-
 599 roshi Saruwatari. Utmos: Utokyo-sarulab system for voicemos challenge 2022. *arXiv preprint*
 600 *arXiv:2204.02152*, 2022.

601 Cees H Taal, Richard C Hendriks, Richard Heusdens, and Jesper Jensen. A short-time objective
 602 intelligibility measure for time-frequency weighted noisy speech. In *2010 IEEE international*
 603 *conference on acoustics, speech and signal processing*, pp. 4214–4217. IEEE, 2010.

605 Chengyi Wang, Sanyuan Chen, Yu Wu, Ziqiang Zhang, Long Zhou, Shujie Liu, Zhuo Chen, Yanqing
 606 Liu, Huaming Wang, Jinyu Li, et al. Neural codec language models are zero-shot text to speech
 607 synthesizers. *arXiv preprint arXiv:2301.02111*, 2023.

608 Dingdong Wang, Junan Li, Mingyu Cui, Dongchao Yang, Xueyuan Chen, and Helen Meng. Speech
 609 discrete tokens or continuous features? a comparative analysis for spoken language understanding
 610 in speechllms. *arXiv preprint arXiv:2508.17863*, 2025a.

612 Xinsheng Wang, Mingqi Jiang, Ziyang Ma, Ziyu Zhang, Songxiang Liu, Linqin Li, Zheng Liang,
 613 Qixi Zheng, Rui Wang, Xiaoqin Feng, et al. Spark-tts: An efficient llm-based text-to-speech
 614 model with single-stream decoupled speech tokens. *arXiv preprint arXiv:2503.01710*, 2025b.

615 Yuncheng Wang, Haoyue Zhan, Liwei Liu, Ruihong Zeng, Haotian Guo, Jiachen Zheng, Qiang
 616 Zhang, Xueyao Zhang, Shunsi Zhang, and Zhizheng Wu. Maskgct: Zero-shot text-to-speech with
 617 masked generative codec transformer. *arXiv preprint arXiv:2409.00750*, 2024.

618 Zhifei Xie and Changqiao Wu. Mini-omni: Language models can hear, talk while thinking in
 619 streaming. *arXiv preprint arXiv:2408.16725*, 2024.

621 Detai Xin, Xu Tan, Shinnosuke Takamichi, and Hiroshi Saruwatari. Bigcodec: Pushing the limits of
 622 low-bitrate neural speech codec. *arXiv preprint arXiv:2409.05377*, 2024.

623 Jin Xu, Zhifang Guo, Jinzheng He, Hangrui Hu, Ting He, Shuai Bai, Keqin Chen, Jialin Wang, Yang
 624 Fan, Kai Dang, et al. Qwen2. 5-omni technical report. *arXiv preprint arXiv:2503.20215*, 2025.

626 Dongchao Yang, Songxiang Liu, Haohan Guo, Jiankun Zhao, Yuanyuan Wang, Helin Wang, Zeqian
 627 Ju, Xubo Liu, Xueyuan Chen, Xu Tan, et al. Almtokenizer: A low-bitrate and semantic-rich audio
 628 codec tokenizer for audio language modeling. *arXiv preprint arXiv:2504.10344*, 2025.

629 Zhen Ye, Peiwen Sun, Jiahe Lei, Hongzhan Lin, Xu Tan, Zheqi Dai, Qiuqiang Kong, Jianyi Chen,
 630 Jiahao Pan, Qifeng Liu, et al. Codec does matter: Exploring the semantic shortcoming of codec
 631 for audio language model. In *Proceedings of the AAAI Conference on Artificial Intelligence*,
 632 volume 39, pp. 25697–25705, 2025a.

633 Zhen Ye, Xinfu Zhu, Chi-Min Chan, Xinsheng Wang, Xu Tan, Jiahe Lei, Yi Peng, Haohe Liu, Yizhu
 634 Jin, Zheqi Dai, et al. Llasa: Scaling train-time and inference-time compute for llama-based speech
 635 synthesis. *arXiv preprint arXiv:2502.04128*, 2025b.

636 Neil Zeghidour, Alejandro Luebs, Ahmed Omran, Jan Skoglund, and Marco Tagliasacchi. Sound-
 637 stream: An end-to-end neural audio codec. *IEEE/ACM Transactions on Audio, Speech, and*
 638 *Language Processing*, 30:495–507, 2021.

640 Ruonan Zhang, Xiaoyang Hao, Yichen Han, Junjie Cao, Yue Liu, and Kai Zhang. Mb-
 641 codec:thorough disentangle for high-fidelity audio compression, 2025. URL <https://arxiv.org/abs/2509.17006>.

643 Xin Zhang, Dong Zhang, Shimin Li, Yaqian Zhou, and Xipeng Qiu. Speechtokenizer: Unified
 644 speech tokenizer for speech large language models. *arXiv preprint arXiv:2308.16692*, 2023a.

645 Ziqiang Zhang, Long Zhou, Chengyi Wang, Sanyuan Chen, Yu Wu, Shujie Liu, Zhuo Chen, Yanqing
 646 Liu, Huaming Wang, Jinyu Li, et al. Speak foreign languages with your own voice: Cross-lingual
 647 neural codec language modeling. *arXiv preprint arXiv:2303.03926*, 2023b.

648 A THE USE OF LARGE LANGUAGE MODELS
649

650 We acknowledge the use of large language models (LLMs), such as OpenAI’s ChatGPT, as a writing-
651 assistance tool during the preparation of this manuscript. The primary use of the LLM was for
652 improving the clarity and readability of the text, correcting grammatical errors, and rephrasing sen-
653 tences. We emphasize that the LLM was used solely for text editing and was not involved in the
654 generation of core scientific ideas, experimental design, data analysis, or the drawing of conclu-
655 sions. All intellectual content, arguments, and the final manuscript were produced by the human
656 authors, who take full responsibility for them.

658 B IMPLEMENTATION DETAILS OF MAPI
659

660 **Input Transformation** We expect that the transformations applied to the input embedding x can
661 significantly influence the output, which avoids excessively similar outputs across different parallel
662 streams. Inspired by (Chen et al., 2025), we utilize random mask strategy to implement input trans-
663 formation. To be specific, we first duplicate the input x into P parallel copies, distinguishing them
664 with different mask segments in each attention layer, which is sufficient to ensure diverse outputs
665 across different streams.

666 **Output Aggregation** As stated in (Chen et al., 2025), dynamic aggregation weights performs better
667 than static ones. Similarly, we concatenate each output together and use an MLP $h : \mathbb{R}^{d \times P} \rightarrow \mathbb{R}^P$
668 to convert it into a vector of length P as aggregation weights. The process can be formalized as:

$$669 \quad w_1, \dots, w_P \leftarrow \text{Softmax}(h(\text{Concat}[\theta_S(\mathbf{z}_1); \dots; \theta_S(\mathbf{z}_P)])), \quad (10)$$

670 where Softmax ensures aggregation weights are normalized, \mathbf{z}_i represents masked input tokens. It
671 can be seen as dynamically weighting different parallel streams during forward process for each
672 token.

675 C MODEL ARCHITECTURE AND TRAINING RECIPE
676677 C.1 MODEL ARCHITECTURE AND SETTING
678

679 **Model Architecture** Our proposed audio codec is a fully convolutional autoencoder consisting of
680 an encoder, a Residual Vector Quantizer (RVQ), and a decoder. The fundamental component of
681 our architecture is a residual block, which contains a strided convolution for dimensionality change
682 (downsampling or upsampling) followed by a stack of convolutional layers. We utilize the non-
683 linear Snake function as the activation throughout these blocks. The encoder is composed of five
684 such blocks, which progressively downsample the input waveform with strides of [2, 4, 5, 6, 8]. The
685 decoder mirrors this structure with five corresponding upsampling blocks with strides of [8, 6, 5, 4,
686 2] and is configured with an internal channel dimension of 2048.

687 **Model Setting** To train the model, we employ a GAN-based objective with a combination of two
688 discriminators: a multi-period discriminator [18] with periods of [2, 3, 5, 7, 11], and a complex
689 multi-scale STFT discriminator. The STFT discriminator operates on three resolutions with window
690 lengths [2048, 1024, 512] and a hop length of 1/4 the window size, using frequency band splits of
691 [0.0, 0.1, 0.25, 0.5, 0.75, 1.0]. The total loss function is a weighted sum of a GAN loss, feature
692 matching loss, a codebook loss, and a multi-resolution reconstruction loss. The reconstruction loss
693 is computed as the L1 distance between the log-mel spectrograms of the original and reconstructed
694 audio over seven different resolutions. These resolutions use window lengths of [32, 64, 128, 256,
695 512, 1024, 2048] with a corresponding number of mel bands [5, 10, 20, 40, 80, 160, 320], respec-
696 tively.

697 C.2 TRAINING OBJECTIVE
698

699 Our model is trained with a multi-task objective that jointly optimizes for reconstruction fidelity and
700 semantic alignment. The primary task is reconstruction, which is guided by a GAN-based objective
701 comprising a reconstruction term, a discriminative loss, and an RVQ commitment loss. This is
complemented by a semantic distillation task, which introduces an additional loss term to ensure

702 the model’s representations are linguistically meaningful. In the following, \mathbf{x} represents an speech
 703 signal and $\hat{\mathbf{x}}$ denotes the reconstructed signal.
 704

705 **Reconstruction Loss** The reconstruction loss comprises a time and a frequency domain loss. For
 706 time domain, we minimize the $L1$ distance between \mathbf{x} and $\hat{\mathbf{x}}$, i.e. $\mathcal{L}_t = \|\mathbf{x} - \hat{\mathbf{x}}\|_1$. For frequency
 707 domain, we use the $L1$ loss over the mel-spectrogram using several time scales. Formally, $\mathcal{L}_f =$
 708 $\sum_{i \in e} \|\mathcal{S}_i(\mathbf{x}) - \mathcal{S}_i(\hat{\mathbf{x}})\|_1$, where \mathcal{S}_i is a 64-bins mel-spectrogram using a normalized STFT with
 709 window size of 2^i and hop length of $2^i/4$, $e = 5, \dots, 11$ is the set of scales.
 710

711 **Discriminator Loss** We use the same discriminator as (Kumar et al., 2023) that consist of three
 712 discriminators. The adversarial loss is used to promote perceptual quality and it is defined as a hinge
 713 loss (Lim & Ye, 2017) over the logits of the discriminator, averaged over multiple discriminators
 714 and over time. Let K denote the number of discriminators. For discriminators, \mathcal{L}_D is defined as :

$$714 \quad \mathcal{L}_D = \frac{1}{K} \sum_{k=1}^K \max(1 + D_k(\hat{\mathbf{x}}), 0) + \max(1 - D_k(\mathbf{x}), 0). \quad (11)$$

715 The adversarial loss for the generator \mathcal{L}_g is constructed as follows:
 716

$$717 \quad \mathcal{L}_g = \frac{1}{K} \sum_{k=1}^K \max(1 - D_k(\hat{\mathbf{x}}), 0). \quad (12)$$

718 Additionally, the feature matching loss for the generator is computed as follow:
 719

$$720 \quad \mathcal{L}_{feat} = \frac{1}{KL} \sum_{K=1}^K \sum_{l=1}^L \frac{\|D_k^l(\mathbf{x}) - D_k^l(\hat{\mathbf{x}})\|_1}{\text{mean}(\|D_k^l(\mathbf{x})\|_1)}, \quad (13)$$

721 where the mean is computed over all dimensions and L is the number of layers in discriminators.
 722

723 **RVQ Commitment Loss** We add a commitment loss \mathcal{L}_w between the pre-quantized value, and
 724 its quantized value, without gradient computed for the quantized value. The commitment loss is
 725 defined as : $\mathcal{L}_w = \sum_{i=1}^{N_q} \|\mathbf{z}_i - \mathbf{z}_{q_i}\|$, where \mathbf{z}_i and \mathbf{z}_{q_i} denote current residual and nearest entry in
 726 the corresponding codebook respectively.
 727

728 The generator is trained to optimize the following loss:
 729

$$730 \quad \mathcal{L}_G = \lambda_t \mathcal{L}_t + \lambda_f \mathcal{L}_f + \lambda_g \mathcal{L}_g + \lambda_{feat} \mathcal{L}_{feat} + \lambda_w \mathcal{L}_w + \lambda_{distill} \mathcal{L}_{distill}, \quad (14)$$

731 where λ_{all} are the hyper-parameters used to balance each loss item. The detailed values are refered
 732 to (Kumar et al., 2023). $\lambda_{distill}$ is set to 0.1 in our work, and $\mathcal{L}_{distill}$ has been described in Section
 733 3.1.1.
 734

735 D TRAINING OBJECTIVE OF CAT-TTS

736 We use the maximum likelihood function to solve this problem.
 737

$$738 \quad \begin{aligned} \mathcal{L}_{total} &= -\log \mathbb{P}(\mathbf{A}|\mathcal{T}, \tilde{\mathbf{A}}) \\ 739 &= -\log \prod_{t=1}^{L_{|S|}} \left[\mathbb{P}(\mathbf{S}_t|\mathbf{S}_{<t}, \mathcal{T}, \tilde{\mathbf{A}}; \theta_S) \cdot \prod_{k=0}^{K-1} \mathbb{P}(\mathcal{A}_t^k|\mathcal{A}_t^{<k}, \mathbf{S}_t; \theta_A) \right] \\ 740 &= -\sum_{t=1}^{L_{|S|}} \log \left[\mathbb{P}(\mathbf{S}_t|\mathbf{S}_{<t}, \mathcal{T}, \tilde{\mathbf{A}}; \theta_S) \cdot \prod_{k=0}^{K-1} \mathbb{P}(\mathcal{A}_t^k|\mathcal{A}_t^{<k}, \mathbf{S}_t; \theta_A) \right] \\ 741 &= -\sum_{t=1}^{L_{|S|}} \left[\log \mathbb{P}(\mathbf{S}_t|\mathbf{S}_{<t}, \mathcal{T}, \tilde{\mathbf{A}}; \theta_S) + \log \prod_{k=0}^{K-1} \mathbb{P}(\mathcal{A}_t^k|\mathcal{A}_t^{<k}, \mathbf{S}_t; \theta_A) \right] \\ 742 &= -\sum_{t=1}^{L_{|S|}} \left[\log \mathbb{P}(\mathbf{S}_t|\mathbf{S}_{<t}, \mathcal{T}, \tilde{\mathbf{A}}; \theta_S) + \sum_{k=0}^{K-1} \log \mathbb{P}(\mathcal{A}_t^k|\mathcal{A}_t^{<k}, \mathbf{S}_t; \theta_A) \right] \\ 743 &= \sum_{t=1}^{L_{|S|}} \left[-\log \mathbb{P}(\mathbf{S}_t|\mathbf{S}_{<t}, \mathcal{T}, \tilde{\mathbf{A}}; \theta_S) - \sum_{k=0}^{K-1} \log \mathbb{P}(\mathcal{A}_t^k|\mathcal{A}_t^{<k}, \mathbf{S}_t; \theta_A) \right]. \end{aligned} \quad (15)$$

756 To be noticed, in Equation 5, we have
 757

$$758 \quad \mathcal{L}_{ctx} = - \sum_{t=1}^{L_{|S|}} \log \mathbb{P}(\mathbf{S}_t | \mathcal{T}, \mathbf{S}_{<t}, \tilde{\mathbf{A}}; \theta_{\mathcal{S}}) \rightarrow \mathcal{L}_{ctx} = \sum_{t=1}^{L_{|S|}} \|\mathbf{S}_t - \theta_{\mathcal{S}}(\mathbf{S}_{<t}, \mathcal{T}, \tilde{\mathbf{A}})\|_2, \quad (16)$$

761 thus the above equation can be transformed as follows:
 762

$$763 \quad \mathcal{L}_{total} = \sum_{t=1}^{L_{|S|}} \left[-\log \mathbb{P}(\mathbf{S}_t | \mathbf{S}_{<t}, \mathcal{T}, \tilde{\mathbf{A}}; \theta_{\mathcal{S}}) - \sum_{k=0}^{K-1} \log \mathbb{P}(\mathcal{A}_t^k | \mathcal{A}_t^{<k}, \mathbf{S}_t; \theta_{\mathcal{A}}) \right] \\ 764 \quad = \mathcal{L}_{total} = \sum_{t=1}^{L_{|S|}} \left[\|\mathbf{S}_t - \theta_{\mathcal{S}}(\mathbf{S}_{<t}, \mathcal{T}, \tilde{\mathbf{A}})\|_2 - \sum_{k=0}^{K-1} \log \mathbb{P}(\mathcal{A}_t^k | \mathcal{A}_t^{<k}, \mathbf{S}_t; \theta_{\mathcal{A}}) \right]. \quad (17)$$

770 E SEMANTIC SUPERIORITY OF S3CODEC

772 E.1 DETAILS OF S3CODEC

774 To discretize waveforms into audio tokens, we introduce S3Codec, a neural audio codec that operates
 775 as an autoencoder with a discrete bottleneck. As Figure 2 shows, S3Codec consists of an autoen-
 776 coder and Residual Vector Quantizer. Based on the DAC architecture (Kumar et al., 2023), the en-
 777 coder projects a single-channel waveform $\mathbf{x} \in \mathbb{R}^T$ to a latent representation $\mathbf{A} = \text{enc}(\mathbf{x}) \in \mathbb{R}^{L \times D}$
 778 by cascading residual convolutional blocks that interleave dilated and strided convolutions along
 779 with Snake nonlinearities and weight normalizaton, and Quantizer quantize the latent representa-
 780 tion to discrete representations $\mathbf{C} \in \mathbb{R}^{K \times L \times D}$ where L represents the length of encoded tokens,
 781 K represents the number of codebooks and D represents the dimension of codebook. Similarly
 782 to SpeechTokenizer and Mimi, we distill semantic information into the first level of RVQ. How-
 783 ever, instead of using SSL models like HuBERT (Hsu et al., 2021) as a semantic teacher, we adopt
 784 Whisper (Radford et al., 2023), a state-of-the-art model for automatic speech recognition and speech
 785 translation whose hidden representation contains rich explicit linguistic features. It projects a 16kHz
 786 waveform into 1280-dimensional embeddings sampled at 50Hz, while S3Codec projects a 24kHz
 787 waveform into 4096-dimensional at 12.5 Hz. During training, we thus downsample the waveforms
 788 and project them to the same dimension as targets for distillation. Mimi (Défossez et al., 2024)
 789 found that, while distillation significantly improves the phonetic discriminability of the first quan-
 790 tizer, it also negatively affects the audio quality. To address the issue, we split the RVQ layers in a
 791 way similar to Mimi. Rather than a single RVQ with K levels, we distill the semantic information
 792 into a plain VQ and apply an RVQ with $K - 1$ levels in parallel. Their outputs will be summed up;
 793 thus the constraint of acoustic information being conserved in the residual of the semantic quantizer
 794 is removed.

794 **Training Loss.** We compute the frequency domain reconstruction loss using L1 loss on multi-
 795 scale mel-spectrograms. Multi-period discriminator and multi-band multi-scale STFT discriminator
 796 are used for waveform discrimination and frequency domain discrimination, respectively. RVQ
 797 codebook learning incorporates both a codebook loss and a commitment loss.

798 **Training Configuration.** All audio samples are 24kHz. The codec has 8 codebooks, each with
 799 4096 entries. For optimization, we use AdamW optimizer with moving average coefficients $\beta_1 =$
 800 0.8 and $\beta_2 = 0.99$. The model converges within approximately 900k training steps using a batch
 801 size of 128.

802 **Evaluation Setup.** To evaluate the preservation of acoustic information, we employ several met-
 803 rics. Speaker similarity (SIM) is calculated as the cosine similarity between speaker embeddings ex-
 804 tracted from original and reconstructed audio using a pre-trained speaker verification model. STFT
 805 and Mel represent the spectrogram distance between original and reconstructed speech. We also use
 806 short-time objective intelligibility (STOI) (Taal et al., 2010) to measure speech intelligibility and
 807 perceptual evaluation of speech quality (PESQ) (Rix et al., 2001) to assess audio quality. All evalua-
 808 tions were conducted on the LibriSpeech (Panayotov et al., 2015) test-clean subset. To demonstrate
 809 the semantic alignment, we trained small CaT-TTS models powered by S3Codec and DAC, respec-
 810 tively.

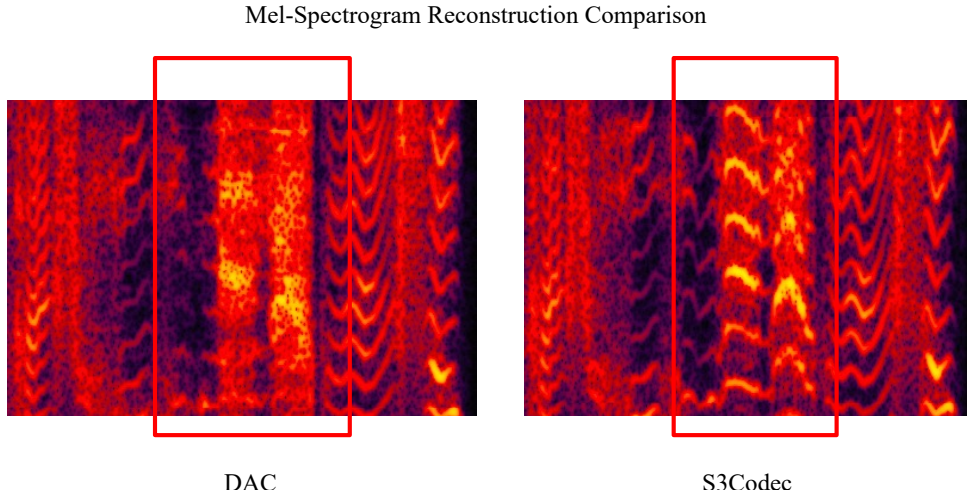


Figure 4: The result analysis of mel-spectrogram reconstruction.

E.2 SEMANTIC PRESERVATION OF S3CODEC

To demonstrate the capability of semantic preservation of S3Codec, we trained CaT-TTS small powered with S3Codec and DAC, respectively. We use WER as the evaluation metric, representing the speech intelligibility of the generated results. Table 5 shows the evaluation results on Seed-TTS test zh easy, PGC-Hard and PGC-Poly. Compared to S3Codec-based system, DAC-based model's performance on speech intelligibility has decreased. The reason lies that DAC dose not contain structured linguistic features as S3Codec, which makes the LM model harder to understand, leading to worse performance than S3Codec.

Model	SeedTTS-test	PGC-Hard	PGC-Poly
DAC-Based	4.21	12.83	19.27
S3Codec-Based	3.30	9.75	16.53

Table 5: Objective Word Error Rate evaluation.

We visualize the mel-spectrogram reconstruction results below. As can be seen, the reconstruction results of S3Codec is more clear, while there exists a blurry segment in the result reconstructed by DAC.

E IMPLEMENTATIONS OF CAT-TTS AND BASELINE DETAILS

F.1 CAT-TTS ARCHITECTURE

Semantic Transformer Semantic Transformer is a decoder-only transformer. The dimension is 1536, with 12 layers.

Acoustic Transformer Acoustic Transformer is also a decoder-only architecture, with 8 layers, and the dimension is 1024.

Text Tokenizer We use the Whisper Tokenizer, with 50260 text vocabularies size.

Regarding the CaT-TTS small, the semantic transformer is 8 decoder-only transformer layers, with 1024 model dimension, and the acoustic transformer is 4 decoder-only transformer layers, with 512 model dimension.

864 F.2 BASELINE DETAILS
865866 **VALL-E (Wang et al., 2023):** AR + NAR TTS system. The first AR model predicts the first
867 codebook, and the second transformer predict the remaining codebooks.868 **Seed-TTS (Anastassiou et al., 2024):** Hybrid TTS system. A two-stage model that employs an AR
869 LM for semantic token prediction and flow matching for acoustic feature generation.870 **FireRedTTS (Guo et al., 2024):** Hybrid TTS system. A two-stage model similar to Seed-TTS,
871 using an AR LM for semantic tokens and flow matching for acoustic features.872 **MaskGCT (Wang et al., 2024):** NAR TTS system. A NAR model that applies masking-based
873 generative strategies for speech synthesis.874 **E2-TTS (Eskimez et al., 2024):** NAR TTS system. A flow matching-based model that predicts Mel
875 spectrograms as acoustic features.876 **F5-TTS (Chen et al., 2024b):** NAR TTS system. A flow matching-based model that predicts Mel
877 spectrograms as acoustic features.878 **CosyVoice series (Du et al., 2024a;b; 2025):** Hybrid TTS system. AR for semantic prediction and
879 flow-matching for acoustic feature generation.880 **Spark-TTS (Wang et al., 2025b):** Single codebook Neural Audio Codec based Pure language TTS
881 model. Powered by BiCodec and Qwen LLM.882 **QTTS (Han et al., 2025):** Pure Codec based language audio model. A two-stage AR+AR model.
883 RVQ-based two stage speech synthesis modeling.884 **Llassa (Ye et al., 2025b):** A single-stream codecbase TTS model that uses a single AR language
885 model for direct single-stream code prediction.886
887
888
889
890
891
892
893
894
895
896
897
898
899
900
901
902
903
904
905
906
907
908
909
910
911
912
913
914
915
916
917